HAL
open science

Magnetoelectric nonlinearity in magnetoelectric laminate sensors

Liangguo Shen, Menghui Li, Junqi Gao, Ying Shen, J.F. Li, D. Viehland, Xin Zhuang, Marc Lam Chok Sing, Christophe Cordier, Sébastien Saez, et al.

To cite this version:

Liangguo Shen, Menghui Li, Junqi Gao, Ying Shen, J.F. Li, et al.. Magnetoelectric nonlinearity in magnetoelectric laminate sensors. Journal of Applied Physics, 2011, 110 (11), pp.114510-1/114510-6. hal-00987001

HAL Id: hal-00987001

https://hal.science/hal-00987001v1

Submitted on 5 May 2014

HAL is a multi-disciplinary open access archive for the deposit and dissemination of scientific research documents, whether they are published or not. The documents may come from teaching and research institutions in France or abroad, or from public or private research centers.

L'archive ouverte pluridisciplinaire **HAL**, est destinée au dépôt et à la diffusion de documents scientifiques de niveau recherche, publiés ou non, émanant des établissements d'enseignement et de recherche français ou étrangers, des laboratoires publics ou privés.

Magnetoelectric nonlinearity in magnetoelectric laminate sensors

Liangguo Shen,[1,a)] Menghui Li,[1] Junqi Gao,[1] Ying Shen,[1] J. F. Li,[1] D. Viehland,[1] X. Zhuang,[2] M. Lam Chok Sing,[2] C. Cordier,[2] S. Saez,[2] and C. Dolabdjian[2]
[1]*Department of Materials Science and Engineering, Virginia Tech, Blacksburg, Virginia 24061, USA*
[2]*Groupe de Recherche en Informatique, Image, Automatique et Instrumentation de Caen (GREYC), CNRS UMR 6072–ENSICAEN and University of Caen, Caen Cedex, 14050, France*

(Received 10 February 2011; accepted 27 October 2011; published online 5 December 2011)

A nonlinearity in the magnetoelectric coefficient, α_{ME}^{Nonlin}, of Metglas/Pb(Zr,Ti)O_3 (PZT) and Metglas/Pb($Mg_{1/3}$,$Nb_{2/3}$)O_3-$PbTiO_3$ (PMN-PT) laminate sensors has been observed. This nonlinearity was found to be dependent on the dc magnetic bias (H_{dc}) and frequency of the ac drive field (H_{ac}). The maximum value of α_{ME}^{Nonlin} for both types of composites was found near the electromechanical resonance. For Metglas/PZT laminates, the maximum occurred under a finite bias of $H_{dc} \approx 5$ Oe; whereas, for Metglas/PMN-PT, the maximum was found near zero dc bias. One application for α_{ME}^{Nonlin} is a cross-modulation scheme that can shift low frequency signals to higher frequency to achieve lower noise floor. For Metglas/PMN-PT, α_{ME}^{Nonlin} has another application: removal of the necessity of a dc bias, which helps to design high-sensitivity sensor arrays and gradiometers.
© *2011 American Institute of Physics*. [doi:10.1063/1.3665130]

I. INTRODUCTION

Recently, there has been much interest in low-frequency ($\approx$1 Hz), low-power, low-cost, room-temperature magnetic sensors with high sensitivity and low equivalent magnetic noise floors.[1,2] There are various types of commercial magnetic sensors that have some of these characteristics, but not all. With regards to high sensitivity and low noise floors, superconducting quantum interference devices (SQUIDs) are the most well-known: but, they need to be operated at cryogenic temperature, which makes the system costly and large.[3] Other smaller and less costly magnetic sensors, such as fluxgates, do not have the required sensitivities and detectable field ranges.[4] They operate at room temperature, but are not truly passive.

To date, magnetic sensors based on the magneto-electric (ME) effect have been widely investigated.[4–10] The ME effect is a polarization response to an applied magnetic field, H; or conversely, a magnetization response to an applied electric field, E.[5] Researchers have found that two-phase laminate composites which contain magnetostrictive and piezoelectric phase layers laminated together have giant ME effects.[6] Generally, the ME response is described by a linear ME voltage coefficient α_{ME}, defined as[5–7]

$$\alpha_{ME} = E/H_{inc}\,[\mathrm{V/cm-Oe}], \tag{1}$$

where H_{inc} is the incident field to be detected. Values of the linear ME voltage coefficient of $\alpha_{ME} = 20$ V/cm − Oe and $\alpha_{ME} = 500$ V/cm − Oe have been reported at low and electromechanical resonance (EMR) frequencies,[7] respectively, for the trilayer laminate of Metglas/Pb(Zr,Ti)O_3 (PZT) /Metglas.

Prior investigations have focused on the linear ME response[4–10] and constitutive equations.[5] However, the individual layers are known to have significant piezoelectric[8] and effective piezomagnetic[9] nonlinearities. Such nonlinearities are known to be extrinsic, and dependent on external variables, such as frequency and dc electric/magnetic fields. These nonlinearities, in the piezoelectric coefficient, have contributions from domain wall dynamics.[10] Different regimes of domain wall dynamics are known under different drive ranges: these include both reversible and irreversible domain wall displacements. In ME laminate systems with significant magnetoelectric coupling, inherent non-linearities induced in one phase should be transferred to the other. An equivalent model for the ME laminate can be reached based on constitutive piezoelectric, piezomagnetic, and motion equations.[5,11] The ME voltage (dV/dH) and ME charge (dQ/dH) coefficients in the L-T mode can be deduced from the 1-D Mason's equivalent model as

$$\frac{dV}{dH} \approx \left(\frac{n(1-n)d_{33,m}g_{31,p}}{n\,s_{11,p}^{E}\left(1-k_{31,p}^{2}\right)+(1-n)s_{33,m}^{H}}\right)t_{lam}\cdot[\mathrm{V/Oe}], \tag{2}$$

$$\frac{dQ}{dH} \approx \left(\frac{d_{33,m}h_{31,p}\varepsilon_{33}^{S}s_{33,m}s_{11,p}}{\left(n\,s_{11,p}+(1-n)s_{33,m}\right)t_{lam}+s_{33,m}s_{11,p}h_{31}^{2}\varepsilon_{33}^{S}lw}\right) \times lwt_{lam}\cdot[\mathrm{C/Oe}], \tag{3}$$

where $s_{11,p}^{E}$ and $s_{33,m}^{H}$ are the elastic compliances of the piezoelectric and magnetostrictive layers, $d_{33,m}$ the effective linear longitudinal piezomagnetic coefficient, $g_{31,p}$ the transverse piezoelectric voltage coefficient, $k_{31,p}$ the piezoelectric coupling coefficient, n the thickness ratio of the piezoelectric and magnetostrictive layers, l and w are length and width of the laminate, and t_{lam} is the total thickness of the laminate.[12] Clearly, these formulas can be extended to nonlinear regimes, given that the piezomagnetic and piezoelectric coefficients involved are allowed to be nonlinear.

The best ME laminate composites, as magnetic sensors, achieve an intrinsic equivalent magnetic noise floor of 20

[a)]Author to whom correspondence should be addressed. Electronic mail: shenliangguo@gmail.com.

 © 2011 American Institute of Physics

Author complimentary copy. Redistribution subject to AIP license or copyright, see http://jap.aip.org/jap/copyright.jsp

pT/$\sqrt{\text{Hz}}$ at 1 Hz in a good laboratory magnetic environment and at room temperature.[13] Fluctuations in low frequency noise (i.e., $1/f^n$, with n as an integer) make further decreases in the noise floor increasingly challenging. Previously, ME sensors have used a charge amplifier (CA) detection method to amplify low frequency magnetic signals.[14] Figure 1 shows a typical noise model for such a ME sensor detection unit, where v_n and i_n are the equivalent input voltage noise and current noise of the charge amplifier,[15] respectively; R_f is the noise generated by the feedback resistor of the charge amplifier; while R_{in} and $\tan(\delta)$ are noises generated by the leakage resistance and dielectric loss factor of the piezoelectric/dielectric layer, respectively. In this graph, it can be seen that the noise floor at low frequency (such as 1 Hz) is around 10 times higher than that at higher frequency (such as 1 kHz).

Three approaches might be taken to mitigate the low frequency magnetic noise floor. The first is to reduce the low frequency noise of the ME sensor detection unit. In this case, the lowest achievable noise floors are limited by physical parameters (R_{in} and $\tan(\delta)$) (Refs. 12 and 15) and the requirement of room-temperature operation. In addition, when operating the sensor in a laboratory environment, external low frequency noises (such as vibration and thermal noises) will also be limiting factors.[15–17] The second approach is to implement a modulation scheme.[18] Such a scheme can only mitigate low frequency noise that exists in the charge amplifier, and thus, the internal noise of the sensor and external low frequency noises will still be limitations.

The third approach is to use a cross-modulation scheme.[12]An implementation of a ME sensor detection unit using such cross modulation can be found in Ref. 12. The low frequency magnetic signal that needs to be detected is an incident field H_{inc} with a frequency of f_1, while a drive field H_{ac} with a frequency of f_0 is applied to the ME sensor using a drive coil. Cross modulation scheme makes use of the nonlinear ME coefficient α_{ME}^{Nonlin} of ME sensors, which is defined as

$$\alpha_{ME}^{Nonlin} = E/(H_{inc} \times H_{ac}) \cdot \left[\text{V/cm} - \text{Oe}^2\right], \tag{4}$$

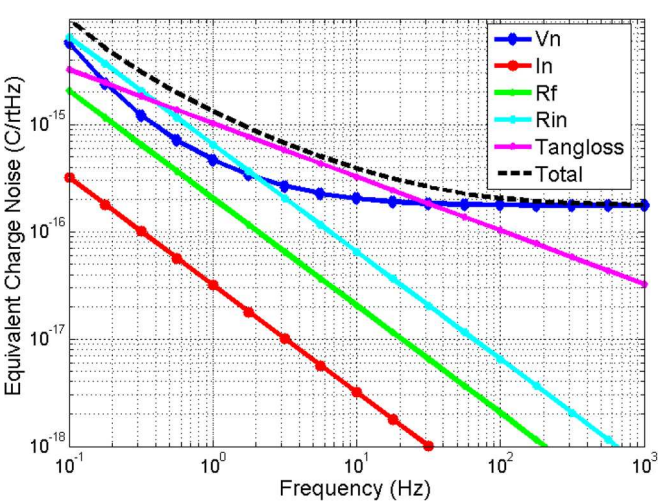

FIG. 1. (Color online) Noise model of charge amplifier based ME sensor detection unit.

where H_{inc} and H_{ac} are the incident and drive fields, respectively. For a linear ME response, there would be no mixing of these two fields. However, if the ME response is nonlinear, then the output signal of the ME sensor will contain cross modulated fields with frequencies of $(f_0 \pm f_1)$. Since f_0 is usually much higher than f_1, the nonlinear ME coefficient α_{ME}^{Nonlin} offers the potential to modulate low frequency magnetic signals (at frequency f_1) to higher frequencies $(f_0 \pm f_1)$, where the noise floor is much lower, as shown in Fig. 1. The potential exists for intrinsic/environmental noise rejection capabilities that exceed those of the charge amplifier detection method, but this potential is not yet realized. Please note that realization of cross-modulation depends on the magnitude of the nonlinear ME coefficients α_{ME}^{Nonlin}, which as noted above have yet to be determined and understood.

In this paper, the nonlinear ME coefficient α_{ME}^{Nonlin} of Metglas/PZT and Metglas/$Pb(Mg_{1/3},Nb_{2/3})O_3$-$PbTiO_3$ (PMN-PT) ME laminates is reported for the first time. We show significant values of α_{ME}^{Nonlin} near the electromechanical resonance frequency for both types of laminates. The maximum value of α_{ME}^{Nonlin} is achieved near zero dc magnetic bias for Metglas/PMN-PT laminates, but under finite biases for Metglas/PZT.

II. EXPERIMENTAL APPROACH

Trilayer ME laminate composites consisting of Metglas and PZT layers, and Metglas and PMN-PT, were fabricated following the procedures previously published.[19] The Metglas foils were obtained from Vacuumschmelze (Hanau, Germany) and were 27 μm in thickness. The foils were cut into a dimension of 8 cm in length and 1 cm in width. The PZT fibers were obtained from Smart Material Corp (Sarasota, FL, USA) and were 170 μm in thickness. Textured PMN-PT fibers were obtained from Ceracomp (Cheonan, Korea) and were of the same thickness. Both types of piezoelectric fibers were cut to a length of 4 cm and a width of 0.2 cm.

In the fabrication of the laminates, we first epoxied three layer stacks of Metglas foils together, following prior reports that resulted in enhanced values of α_{ME}.[18] We then deposited Inter-Digitade (ID) electrodes on both sides of the piezoelectric layer which consisted of 5 fibers. Kapton insulating layers were then epoxied on top of both sides. Finally, we assembled ME laminates by bonding 3-layer Metglas stacks on each side of the piezoelectric fiber.

The magnetostriction was characterized by a strain gauge method, where the strain induced by an applied dc magnetic bias was measured by a strain gauge bridge module BCM-1 (Omega: Stamford, CT, USA). The effective piezomagnetic coefficient was then simply calculated from the derivative of the magnetostriction. We next measured the linear magnetoelectric coefficient α_{ME} using a method previously published.[20] In this method, the voltage induced across the piezoelectric by application of an ac magnetic field was measured at various frequencies and dc magnetic biases.

Finally, we measured the nonlinear ME coefficient α_{ME}^{Nonlin}. We applied both an incident field at a frequency f_1 using a Helmholtz coil and a drive field at a frequency f_0 using a drive coil, and then measured the cross-modulation

Author complimentary copy. Redistribution subject to AIP license or copyright, see http://jap.aip.org/jap/copyright.jsp

fields having frequencies of $(f_0 \pm f_1)$ using an SR-785 dynamic signal analyzer (Stanford Research Systems: Sunnyvale, CA). We converted the cross-modulation fields to α_{ME}^{Nonlin} (with unit of V/cm-Oe^2): which was done by knowing the applied incident and drive fields, and the spacing of the ID electrodes. The cross-modulation fields $(f_0 \pm f_1)$ were then demodulated to a low frequency f_1 using an SR-850 lock-in amplifier. Experimentally, we observed the demodulated signal both using an SR-785 (in frequency domain) and an oscilloscope (in time domain). Please note that the carrier frequency reduction technique mentioned in Ref. 12 was needed to reduce the magnitude of the carrier signal at the drive field frequency of f_0.

III. RESULTS AND DISCUSSION

Figure 2 shows the magnetostriction and effective linear piezomagnetic coefficient of the Metglas/PZT and Metglas/PMN-PT laminates for dc magnetic biases between -50 Oe and 50 Oe. As previously reported,[19] and as can be seen in equations (2) and (3), it is actually not the magnetostriction coefficient that is important to the value of α_{ME}, but rather that of effective linear piezomagnetic coefficient $d_{33,m}$. In this figure, the values of the magnetostriction and $d_{33,m}$ can be seen to be nearly the same for both types of laminates. However, some difference in $d_{33,m}$ can be seen between them at lower values of dc bias field H_{dc}. The changes in magnetostriction with H_{dc} were larger near $H_{dc} = 0$ for the Metglas/PMN-PT laminate than for the Metglas/PZT.

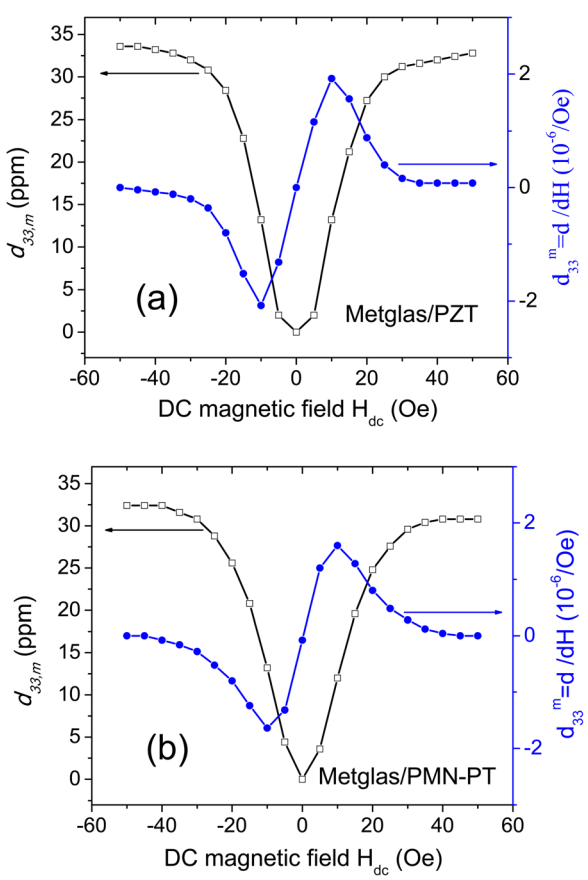

FIG. 2. (Color online) Magnetostriction and piezomagnetic properties of (a) Metglas/PZT and (b) Metglas/PMN-PT sensors.

Figures 3(a) and 3(b) show the linear ME voltage coefficient α_{ME} as a function of H_{dc} for the Metglas/PZT and Metglas/PMN-PT laminates, respectively. The frequency of the incident field H_{inc} was fixed at $f = 1$ kHz, but three different magnitudes of H_{inc} (0.1 Oe, 1 Oe, and 4 Oe) were applied. In these figures, a notable difference in the slope of α_{ME} near $H_{dc} = 0$ can be seen. For the laminate with PZT fibers, two different slope regimes were found for $H_{dc} \leq |\pm 8\ \text{Oe}|$ (as identified by I and II in Fig. 3(a)). In particular, the slope near $H_{dc} = 0$ was much smaller. Whereas, for the laminate with PMN-PT single crystal fibers, no such regime of low slope was observed, rather only a single regime was found for $H_{dc} \leq |\pm 8\ \text{Oe}|$ that had a higher slope. These differences will result in important corresponding differences in the nonlinear ME coefficient α_{ME}^{Nonlin} between the two types of laminate, as will be shown below. In addition, Figs. 3(a) and 3(b) reveal some dependence of α_{ME} on H_{inc}. Prior investigations have not shown such a dependence on H_{inc}. Our findings indicate an inherent nonlinearity in α_{ME}.

Further investigations of the nonlinearity of α_{ME} under different dc magnetic biases was then performed, as summarized in Figs. 3(c) and 3(d) for Metglas/PZT and Metglas/PMN-PT laminates, respectively. The magnitude of the incident field H_{inc} was varied between 0.2 Oe and 4 Oe. Five different H_{dc} biases were chosen: 9.5 Oe (maximum α_{ME} value), 4.8 Oe, 3 Oe, 2 Oe, and 1 Oe. If α_{ME} lacks nonlinearity, then at a given H_{dc}, α_{ME} should be constant and independent of the incident field used. In other words, $\alpha_{ME}/\alpha_{ME}^{Norm}$ should always be equal to one over the entire H_{inc} range, where α_{ME}^{Norm} is the value under $H_{inc} = 0.2$ Oe. However, Figs. 3(c) and 3(d) show that $\alpha_{ME}/\alpha_{ME}^{Norm}$ does change with H_{inc}. The results demonstrate that α_{ME} for both Metglas/PZT and Metglas/PMN-PT laminates are nonlinear. Also, the nonlinearity in α_{ME} was mostly determined by the value of H_{dc}. It is important to note that the nonlinearity was minimal under $H_{dc} = 9.5$ Oe, where α_{ME} was maximum (compare with Figs. 3(a) and 3(b)) for both laminate types, respectively. These findings clearly establish that the nonlinearities are largest at lower bias levels, where the linear α_{ME} is small.

Next, we directly measured the nonlinear ME voltage coefficient α_{ME}^{Nonlin}. These measurements were performed using the cross-modulation method discussed in Sec. II, where the incident field H_{inc} had a frequency of $f_1 = 1$ Hz. Figure 4(a) shows α_{ME}^{Nonlin} for a Metglas/PZT laminate taken at $f_0 = 1$ kHz. A small nonlinearity of $\alpha_{ME}^{Nonlin} = 0.1$ V/cm-Oe^2 was found for $H_{dc} = 9.5$ Oe, near which bias field the linear coefficient α_{ME} was maximum. Please note that previous publications were based on this dc bias field to achieve an optimized operation point.[5–10] However, a maximum nonlinearity of $\alpha_{ME}^{Nonlin} = 1.2$ V/cm-Oe^2 was found under $H_{dc} = 4.8$ Oe. These results clearly demonstrate that an improvement of α_{ME}^{Nonlin} by a factor of $10\times$ can be achieved by optimizing H_{dc}. Figure 4(b) shows α_{ME}^{Nonlin} for a Metglas/PZT sensor taken near its EMR at $f_0 = 31$ kHz. Under this drive condition, a maximum value of α_{ME}^{Nonlin}=25.5 V/cm-Oe^2 was found: which is a $20\times$ improvement compared to that at $f_0 = 1$ kHz. Therefore, for the Metglas/PZT sensor, a total improvement of $255\times$ was achieved by optimizing H_{dc} and f_0.

Author complimentary copy. Redistribution subject to AIP license or copyright, see http://jap.aip.org/jap/copyright.jsp

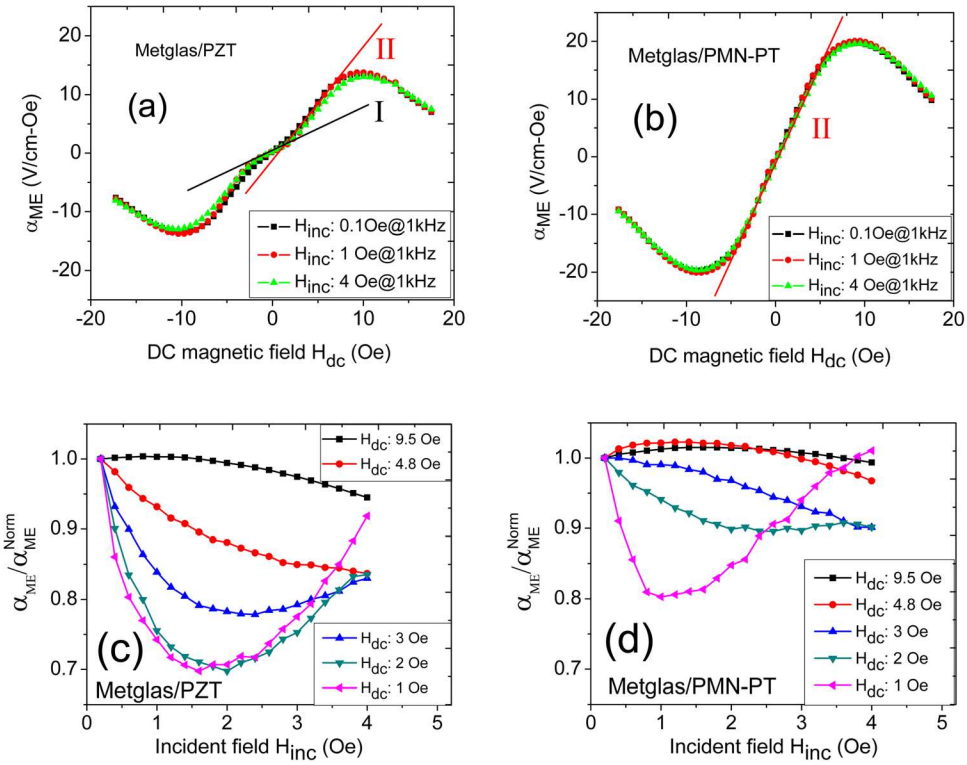

FIG. 3. (Color online) α_{ME} vs H_{dc} curves for (a) Metglas/PZT and (b) Metglas/PMN-PT sensors; $\alpha_{ME}/\alpha_{ME}^{Norm}$ vs H_{inc} curves for (c) Metglas/PZT and (d) Metglas/PMN-PT sensors.

Figures 4(c) and 4(d) show similar measurements of α_{ME}^{Nonlin} for a Metglas/PMN-PT laminate at different frequencies. For $f_0 = 1$ kHz (see Fig. 4(c)), a minimum value of $\alpha_{ME}^{Nonlin} = 0.1$ V/cm-Oe^2 was found near $H_{dc} = 9.5$ Oe, whereas a much larger value of α_{ME}^{Nonlin}=2.2 V/cm-Oe^2 was found under $H_{dc} = 2$ Oe. For $f_0 = 29.5$ kHz near the EMR (see Fig. 4(d)), this maximum value of α_{ME}^{Nonlin} was increased to 25.3 V/cm-Oe.^{2} These results demonstrate a 253 times higher α_{ME}^{Nonlin} which was achieved by optimizing H_{dc} and f_0.

Furthermore, inspection of Figs. 4(c) and 4(d) will reveal that α_{ME}^{Nonlin} is nearly maximum under $H_{dc} = 0$ Oe for Metglas/PMN-PT laminates: this result is much different than that for laminates with PZT fibers, where α_{ME}^{Nonlin} was greatly reduced near $H_{dc} = 0$ Oe. These findings could have significant ramifications to the use of cross-modulation as detection methods for reduced noise, if the intrinsic sensor noise is not measured under an external dc magnetic bias. Not only can the low frequency noise floor be reduced for

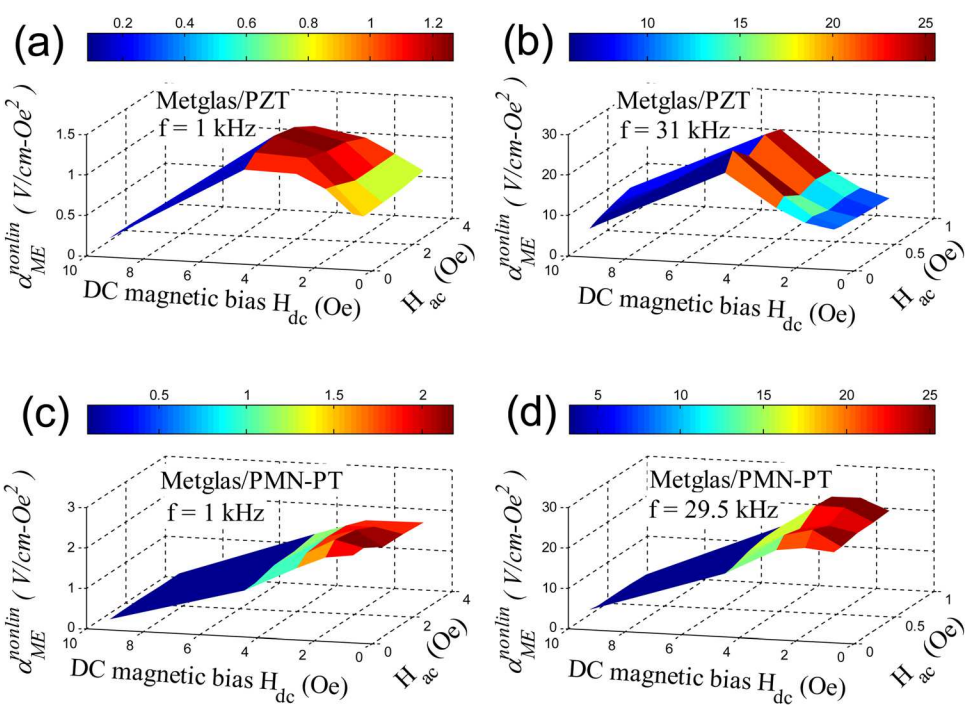

FIG. 4. (Color online) α_{ME}^{Nonlin} optimization of Metglas/PZT sensor at (a) $f_0 = 1$ kHz and (b) $f_0 = 31$ kHz (EMR). α_{ME}^{Nonlin} optimization of Metglas/PMN-PT sensor at (c) $f_0 = 1$ kHz and (d) $f_0 = 29.5$ kHz (EMR), respectively.

Author complimentary copy. Redistribution subject to AIP license or copyright, see http://jap.aip.org/jap/copyright.jsp

Metglas/PMN-PT by cross-modulation, but in addition its maximum performance can be designed to occur without a restriction of having a permanent H_{dc}. The physical reason for this difference in α_{ME}^{Nonlin} between various piezoelectric materials is interesting and should be noted. Single crystals of PMN-PT oriented and poled along [001] are in a domain-engineered state,[21] which has a bridging monoclinic structure.[22,23] Hysteretic and dielectric losses are extremely small under both moderate bipolar and large unipolar drives in this domain engineered state,[24] and thus minor hysteresis loops are negligible under these conditions. Application of the electric field does not result in domain wall motion, but rather the polarization is free to rotate in a plane.[25] However, in conventional PZT piezoelectric ceramics, hysteretic losses are high and minor hysteresis loops known about $E = 0$ in the poled condition.[24] Application of the electric field results in domain movement, where the field at which motion is induced can be notably influenced (i.e., pinned) by substituents and vacancies.

Figure 5 gives the test results for the Metglas/PMN-PT sensor using the cross-modulation scheme, where a 10 nT incident field at a frequency of $f_1 = 1$ Hz and a 0.5 Oe driving field at a frequency of $f_0 = 29.5$ kHz were applied. More information on the cross-modulation approach can be found in Ref. 12. Similar results were found for Metglas/PZT sensors, and thus are not shown: the only difference was that the Metglas/PMN-PT sensors did not need a dc magnetic bias H_{dc} to achieve an optimized value of α_{ME}^{Nonlin}. Figure 5(a) shows the sensor output signal before demodulation, which contains the carrier and cross-modulation signals at the frequencies of 29.5 kHz (f_0), 29.499 kHz, and 29.501 kHz ($f_0 \pm f_1$). Figure 5(b) gives the demodulated 1 Hz magnetic field signal, as obtained by the SR-785 dynamic signal analyzer. This figure shows that the cross-modulation scheme has the ability of transferring low frequency magnetic signal (1 Hz) to higher frequencies (29.499 kHz and 29.501 kHz), where the noise floor is much lower than that at low frequency.[26] Please note that the effectiveness of this frequency transfer is proportional to the nonlinear ME coefficient α_{ME}^{Nonlin}. This is the reason why in this paper we tried to determine the conditions under which the nonlinear ME coefficient α_{ME}^{Nonlin} was maximized.

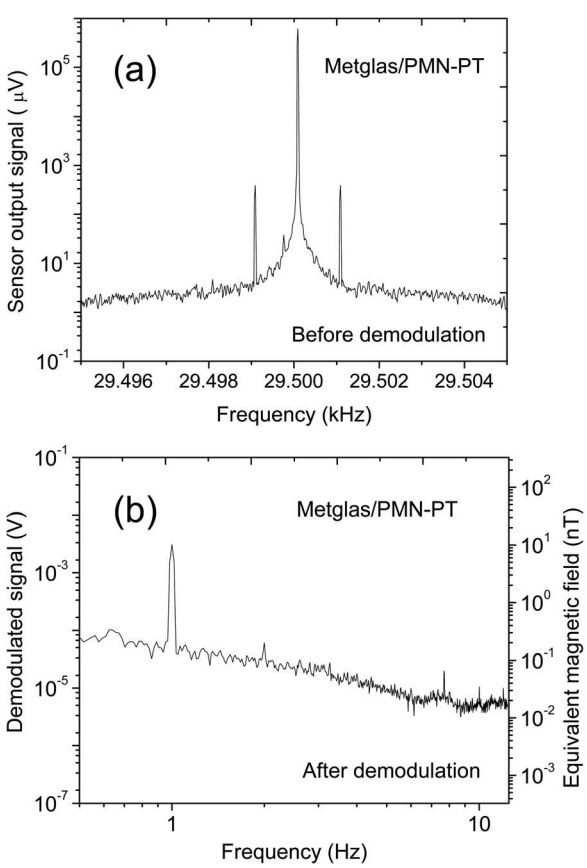

FIG. 5. Demonstrated test results of Metglas/PMN-PT sensors using cross-modulation scheme under $H_{dc} = 0$ Oe: (a) Sensor output signal before demodulation; (b) demodulated 1 Hz signal.

Again, please bear in mind that the results in Fig. 5 were taken with no applied dc magnetic bias H_{dc}. Since no dc bias is needed for the Metglas/PMN-PT sensor, it is a good candidate for sensor array and gradiometer applications,[27,28] because there would be no dc magnetic bias interface among different sensors and therefore the sensor arrangement could be expected to be more flexible.

IV. SUMMARY

We have performed an investigation of the nonlinear magnetoelectric properties of Metglas/PZT and Metglas/PMN-PT sensors. By optimizing H_{dc} and the drive frequency f_0, the nonlinear ME coefficient α_{ME}^{Nonlin} was increased by more than 250 times. We find that the value of α_{ME}^{Nonlin} is large under small H_{dc}, where the linear coefficient α_{ME} is small; whereas, it is small under the bias where linear coefficient α_{ME} is maximum. We also find an important difference between laminates containing PMN-PT fibers as compared to those with PZT ones. This is that those with PZT fibers only have small values of α_{ME}^{Nonlin} near $H_{dc} = 0$ Oe, but those with PMN-PT have maximum values under this condition. The lack of dc bias requirements makes Metglas/PMN-PT sensors a good choice for applications that restrictions with regards to dc bias interference. Using the enhanced nonlinearity found in this study, together with a cross-modulation scheme recently reported,[12] we have been able to reject low frequency noise in laminates, while not requiring dc magnetic biases.

ACKNOWLEDGMENTS

We acknowledge the support from the Defense Advanced Research Projects Agency (DARPA - BAA08 - 70) and assistance from Dr. Keith McLaughlin of SAIC.

[1]See http://www.darpa.mil/dso/solicitations/baa08-70.html for information about DARPA-BAA08-70, Heterostructural Uncooled Magnetic Sensors (HUMS).
[2]D. Robbes, C. Dolabdjian, S. Saez, Y. Monfort, G. Kaiser, and P. Ciereanu, IEEE Trans. Appl. Supercond. **11**, 629 (2001).
[3]J. Vrba, *SQUID Sensors: Fundamentals, Fabrication and Applications*, edited by H. Weinstock (Kluwer Academic, Dordrecht, The Netherlands, 1996), p. 117.
[4]R. H. Koch, J. G. Deak, and G. Grinstein, Appl. Phys. Lett. **75**, 3862 (1999).

Author complimentary copy. Redistribution subject to AIP license or copyright, see http://jap.aip.org/jap/copyright.jsp

[5]L.D. Landau and E. Lifshitz, *Electrodynamics of Continuous Media* (Pergamon, Oxford, 1960), p. 119.
[6]S. X. Dong, J.-F. Li, and D. Viehland, IEEE Trans. Ultrason. Ferroelectr. Freq. Control **50**, 1253 (2003).
[7]S. X. Dong, J. Y. Zhai, J.-F. Li, and D. Viehland, Appl. Phys. Lett. **89**, 252904 (2006).
[8]S. Trolier-McKinstry, N. Bassiri Gharb, and D. Damjanovic, Appl. Phys. Lett. **88**, 202901 (2006).
[9]S. X. Dong, J. Y. Zhai, J.-F. Li, and D. Viehland, Appl. Phys. Lett. **89**, 122903 (2006).
[10]M. Kläui, J. Phys. Condensed Matter **20**, 313001 (2008).
[11]Ce-Wen Nan, Phys. Rev. B **50**, 6082 (1994).
[12]X. Zhuang, M. Lam Chok Sing, C. Cordier, S. Saez, C. Dolabdjian, L. Shen, J. F. Li, M. Li, and D. Viehland, IEEE Sens. J. **11**, 2266 (2011).
[13]J. Y. Zhai, Z. P. Xing, S. Dong, J. F. Li, and D. Viehland, Appl. Phys. Lett. **88**, 062510 (2006).
[14]Z. P. Xing, J. Y. Zhai, S. X. Dong, J. F. Li, D. Viehland, and W. G. Odendaal, Meas. Sci. Technol. **19**, 015206 (2008).
[15]X. Zhuang, M. Lam Chok Sing, C. Cordier, S. Saez, C. Dolabdjian, J. Das, J. Gao, J. F. Li and D. Viehland, IEEE Sens. J. **11**, 2183 (2011).
[16]J. Y. Zhai, Z. P. Xing, S. Dong, J. F. Li, and D. Viehland, Appl. Phys. Lett. **93**, 072906 (2008).
[17]Z. Xing, J. Zhai, J. F. Li, and D. Viehland, J. Appl. Phys. **106**, 024512 (2009).
[18]C. C. Enz, E. A. Vittoz, and F. Krummenacher, IEEE J. Solid-State Circuits **SC-22**, 335 (1987).
[19]J. Das, J. Gao, Z. Xing, J.F. Li, and D. Viehland, Appl. Phys. Lett. **95**, 092501 (2009).
[20]J. Zhai, Z. Xing, S. Dong, J. F. Li, and D. Viehland, J. Am. Ceram. Soc. **91**, 351 (2008).
[21]S. Park and T. Shrout, J. Appl. Phys. **82**, 1804 (1997).
[22]B. Noheda, Z. Zhong, D. Cox, G. Shirane, S. Park, and P. Rehrig, Phys. Rev. B **65**, 224101 (2002).
[23]H. Cao, F. Bai, N. Wang, J. F. Li, D. Viehland, G. Xu, and G. Shirane, Phys. Rev. B **72**, 064104 (2005).
[24]D. Viehland, J. Am. Ceram. Soc. **89**, 775 (2006).
[25]D. Vanderbilt and M. Cohen, Phys. Rev. B **63**, 094108 (2001).
[26]J. Gao, L. Shen, Y. Wang, D. Gray, J. F. Li, and D. Viehland, J. Appl. Phys. **109**, 074507 (2011).
[27]Y. Shen, J. Gao, L. Shen, D. Gray, J. Li, P. Finkel, D. Viehland, X. Zhuang, S. Saez, and C. Dolabdjian, Sensors and Actuators A: Physical **171**, 63 (2011).
[28]J. Gao, J. Zhai, Y. Shen, L. Shen, D. Gray, J. F. Li, P. Finkel, and D. Viehland, IEEE Trans. Ultrason. Ferroelectr. Freq. Control **58**, 1541 (2011).

Author complimentary copy. Redistribution subject to AIP license or copyright, see http://jap.aip.org/jap/copyright.jsp